Numerical modelling of steel beam-columns in case of fire—comparisons with Eurocode 3

P.M.M. Vila Real[a],*, N. Lopes[a], L. Simões da Silva[b], P. Piloto[c], J.-M. Franssen[d]

[a] Department of Civil Engineering, University of Aveiro, Aveiro 3810, Portugal
[b] Department of Civil Engineering, University of Coimbra, Coimbra 3030-290, Portugal
[c] Department of Mechanical Engineering, Polytechnic of Bragança, Bragança, Portugal
[d] Department M&S, University of Liege, Liege, Belgium

Abstract

This paper presents a numerical study of the behaviour of steel I-beams subjected to fire and a combination of axial force and bending moments. A geometrical and material non-linear finite element program, specially established in Liege for the analysis of structures submitted to fire, has been used to determine the resistance of a beam-column at elevated temperature, using the material properties of Eurocode 3, part 1–2. The numerical results have been compared with those obtained with the Eurocode 3, part 1–2 (1995) and the new version of the same Eurocode (2002).

The results have confirmed that the new proposal for Eurocode 3 (2002) is more conservative than the ENV-EC3 (1995) approach.
© 2003 Elsevier Ltd. All rights reserved.

Keywords: Beam-column; Buckling; Torsional-buckling; Fire; Eurocode 3; Numerical modelling

1. Introduction

Under fire conditions, axially and eccentrically loaded columns were studied by Franssen et al. [1–3] for the cases where the failure mode is in the plane of loading, who proposed a procedure for the design of columns under fire loading, later adopted by EC3 [4]. Analogously, Vila Real et al. [5–7] studied the problem of lateral

---

Nomenclature

A	area of the cross-section
E	Young's modulus of elasticity
f_y	yield strength
K	stiffness of the spring
K_v	axial stiffness of the beam
K_{v0}	axial stiffness of the beam at room temperature
$k_{y,\theta}$	reduction factor for the yield strength at temperature, θ_a
$k_{E,\theta}$	reduction factor for the slope of the linear elastic range at temperature, θ_a
M_{SAFIR}	buckling resistance moment in the fire design situation given by SAFIR
$M_{y,fi,Ed}$	design bending moment about y-axis for the fire design situation
$M_{y,fi,\theta,Rd}$	design moment resistance about y-axis of a Class 1 or 2 cross-section with a uniform temperature, θ_a
$N_{fi,Ed}$	design axial force for the fire design situation
$N_{fi,\theta,Rd}$	design axial force resistance with a uniform temperature, θ_a
$W_{el,y}$	elastic section modulus in y-axis
$W_{pl,y}$	plastic section modulus in y-axis

Greek letters

α	imperfection factor and thermal elongation coefficient of steel
$\beta_{M,LT}$	the equivalent uniform moment factor corresponding to lateral-torsional buckling, in this case ($\beta_{M,LT} = \beta_{M,y} = 1.1$)
$\beta_{M,y}$	the equivalent uniform moment factor for the y-axis, in this case ($\beta_{M,y} = 1.1$)
γ_{M0}	partial safety factor (usually $\gamma_{M0} = 1.0$)
$\gamma_{M,fi}$	partial safety factor for the fire situation (usually $\gamma_{M,fi} = 1.0$)
$\bar{\lambda}_{LT}$	non-dimensional slenderness for lateral-torsional buckling at room temperature
$\bar{\lambda}_y$	non-dimensional slenderness of the y-axis for flexural buckling at room temperature
$\bar{\lambda}_z$	non-dimensional slenderness of the z-axis for flexural buckling at room temperature
$\bar{\lambda}_{LT,\theta}$	non-dimensional slenderness for lateral-torsional buckling at temperature, θ_a
$\bar{\lambda}_{y,\theta}$	non-dimensional slenderness of the y-axis for flexural buckling at temperature, θ_a
$\bar{\lambda}_{z,\theta}$	non-dimensional slenderness of the z-axis for flexural buckling at temperature, θ_a
$\chi_{LT,fi}$	reduction factor for lateral-torsional buckling in the fire design situation
$\chi_{min,fi}$	the minimum reduction factor of the y- and z-axis for flexural buckling in the fire design situation

$\chi_{y,\mathrm{fi}}$	the reduction factor of the y-axis for flexural buckling in the fire design situation
$\chi_{z,\mathrm{fi}}$	the reduction factor of the z-axis for flexural buckling in the fire design situation

torsional buckling of beams under fire loading, and proposed a design expression which was also adopted by EC3 [4].

The 3D behaviour of members submitted to combined moment and axial loads, i.e. the interaction between bending, buckling and lateral torsional buckling, was never specifically studied and it is thus impossible to establish the level of safety and accuracy provided by the current design proposals. It is the objective of the present paper to address this issue, using a numerical approach.

2. Numerical model

2.1. Basic hypothesis

The program SAFIR [8], which was chosen to carry out the numerical simulations, is a finite element code for geometrical and material non-linear analysis, specially developed for studying structures in case of fire. In the numerical analyses, a three-dimensional (3D) beam element has been used. It is based on the following formulations and hypotheses:

- Displacement type element in a total co-rotational description;
- Prismatic element;
- The displacement of the node line is described by the displacements of the three nodes of the element, two nodes at each end supporting seven degrees of freedom, three translations, three rotations and the warping amplitude, plus one node at the mid-length supporting one degree of freedom, namely the non-linear part of the longitudinal displacement;
- The Bernoulli hypothesis is considered, i.e., in bending, plane sections remain plane and perpendicular to the longitudinal axis and no shear deformation is considered;
- No local buckling is taken into account, which is the reason why only Class 1 and Class 2 sections can be used [9];
- The strains are small (von Kármán hypothesis), i.e.

$$\frac{1}{2}\frac{\partial u}{\partial x} \ll 1 \tag{1}$$

where u is the longitudinal displacement and x is the longitudinal co-ordinate;
- The angles between the deformed longitudinal axis and the undeformed but translated longitudinal axis are small, i.e.,

$$\sin \varphi \cong \varphi \quad \text{and} \quad \cos \varphi \cong 1$$

where φ is the angle between the arc and the cord of the translated beam finite element;
- The longitudinal integrations are numerically calculated using Gauss' method;
- The cross-section is discretised by means of triangular or quadrilateral fibres. At every longitudinal point of integration, all variables, such as temperature, strain, stress, etc., are uniform in each fibre;
- The tangent stiffness matrix is evaluated at each iteration of the convergence process (pure Newton–Raphson method);
- Residual stresses are considered by means of initial and constant strains [10];
- The material behaviour in case of strain unloading is elastic, with the elastic modulus equal to the Young's modulus at the origin of the stress–strain curve. In the same cross-section, some fibres that have yielded may therefore exhibit a decreased tangent modulus because they are still on the loading branch, whereas, at the same time, some other fibres behave elastically. The plastic strain is presumed not to be affected by a change in temperature [11];
- The elastic torsional stiffness at 20°C that is calculated by the code has been adapted in an iterative process in order to reflect the decrease of material stiffness at the critical temperature [12].

2.2. Case study

A simply supported beam with fork supports was chosen to explore the validity of the beam-column safety verifications, loaded with uniform moment in the major axis and axial compression (Fig. 1). An IPE 220 of steel grade S 235 was used, with a uniform temperature distribution in the cross-section.

A lateral geometric imperfection given by the following expression was considered:

$$y(x) = \frac{l}{1000} \sin \left(\frac{\pi x}{l} \right). \tag{2}$$

Finally, the residual stresses adopted are constant across the thickness of the web and of the flanges. Triangular distribution as in Fig. 2, with a maximum value of 0.3×235 MPa, for the S235 steel has been used [13].
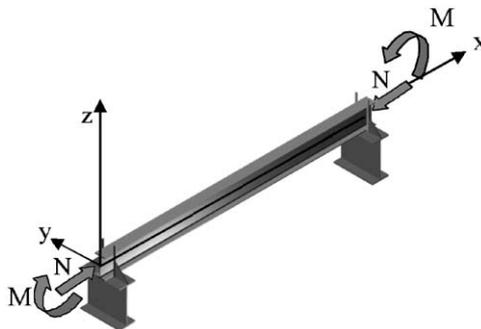

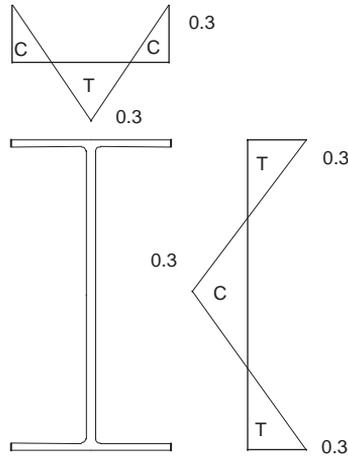Fig. 1. Simply supported beam with bending and axial compression.

Fig. 2. Residual stresses: C—compression; T—tension.

3. The Eurocode models for bending and axial force under fire loading

3.1. Introduction

The Eurocode 3 code provisions for beam-columns under fire loading are based on the corresponding expressions for cold design [9] and consist of interaction formulae between bending moments and axial force [16]. Currently, two alternative versions of Part 1.2 of Eurocode 3 coexist, the ENV version from 1995 [14] and the draft EN version from 2002 [4] that, although being formally identical, yield distinct results because of different calibration coefficients. Both formulae are presented in detail below.

3.2. Simple model according to ENV version of Eurocode 3 (1995)

According to part 1–2 of the Eurocode 3 [4], elements with cross-sectional classes 1 and 2 submitted to bending and axial compression, in case of fire, must satisfy the following condition:

$$
\frac{N_{\mathrm{fi,Ed}}}{(\chi_{\mathrm{min,fi}}/1.2)Ak_{\mathrm{y},\theta}(f_{\mathrm{y}}/\gamma_{M,\mathrm{fi}})}
+ \frac{K_y M_{y,\mathrm{fi,Ed}}}{W_{\mathrm{pl},y}k_{\mathrm{y},\theta}\,(f_{\mathrm{y}}/\gamma_{M,\mathrm{fi}})} \leqslant 1,
\tag{3}
$$

where

$$
K_y = 1 - \frac{\mu_y N_{\mathrm{fi,Ed}}}{(\chi_{y,\mathrm{fi}}/1.2)Ak_{\mathrm{y},\theta}f_{\mathrm{y}}} \quad \text{but} \quad K_y \leqslant 1.5
\tag{4}
$$

and

$$\mu_y = \bar{\lambda}_{y,\theta}(2\beta_{M,y} - 4)\left[\frac{(W_{\text{pl},y} - W_{\text{el},y})}{W_{\text{el},y}}\right]$$
$$\text{but} \quad \mu \leqslant 0.9, \tag{5}$$

where $\chi_{\text{min,fi}}$ is the minimum reduction factor of the axis yy and zz; $W_{\text{pl},y}$ the plastic modulus in axis yy; $k_{y,\theta}$ the reduction factor of the yield strength at temperature θ; $\gamma_{M,\text{fi}}$ the partial safety coefficient in case of fire (usually $\gamma_{M,\text{fi}} = 1$); $\beta_{M,y}$ the equivalent uniform moment factor, in this case ($\beta_{M,y} = 1.1$).

The reduction factor is calculated with the expressions from the part 1.1 of Eurocode 3 [9]. The reduction factor in case of fire, $\chi_{y,\text{fi}}$ *and* $\chi_{z,\text{fi}}$, are determined like at room temperature using the slenderness $\bar{\lambda}_{y,\theta}$ e $\bar{\lambda}_{z,\theta}$ given by Eq. (6). The constant 1.2 is an empirical correction factor. In the calculation of the reduction factor in case of fire the buckling curve used is the curve c ($\alpha = 0.49$):

$$\bar{\lambda}_{y,\theta} = \bar{\lambda}_y\sqrt{\frac{k_{y,\theta}}{k_{E,\theta}}}, \quad \bar{\lambda}_{z,\theta} = \bar{\lambda}_z\sqrt{\frac{k_{y,\theta}}{k_{E,\theta}}}, \tag{6}$$

where $\bar{\lambda}_y$ e $\bar{\lambda}_z$ are the slenderness of the axis yy and zz at room temperature; $k_{E,\theta}$ is the reduction factor of the elastic modulus at temperature θ.

The following values are also defined:

$$N_{\text{fi},\theta,\text{Rd}} = Ak_{y,\theta}\frac{f_y}{\gamma_{M,\text{fi}}}, \quad M_{y,\text{fi},\theta,\text{Rd}} = W_{\text{pl},y}k_{y,\theta}\frac{f_y}{\gamma_{M,\text{fi}}}. \tag{7}$$

In order to compare results, the maximum value of the design moment is divided by the plastic moment resistance at temperature θ. Solving Eq. (3) for $M_{y,\text{fi},\text{Ed}}$ and dividing by $M_{y,\text{fi},\theta,\text{Rd}}$ from Eq. (7), yields

$$\frac{M_{y,\text{fi},\text{Ed}}}{M_{y,\text{fi},\theta,\text{Rd}}} \leqslant \frac{1}{\left(1 - \dfrac{\mu_y N_{\text{fi},\text{Ed}}}{(\chi_{y,\text{fi}}/1.2)N_{\text{fi},\theta,\text{Rd}}\gamma_{M,\text{fi}}}\right)}$$
$$\times \left(1 - \frac{N_{\text{fi},\text{Ed}}}{(\chi_{\text{min,fi}}/1.2)N_{\text{fi},\theta,\text{Rd}}}\right). \tag{8}$$

In addition, also from part 1.2 of EC3 [14], a second condition related to lateral-torsional buckling is also required, and the following formula must also be verified:

$$\frac{N_{\text{fi},\text{Ed}}}{(\chi_{z,\text{fi}}/1.2)Ak_{y,\theta}(f_y/\gamma_{M,\text{fi}})}$$
$$+ \frac{K_{\text{LT}}M_{y,\text{fi},\text{Ed}}}{(\chi_{\text{LT}}/1.2)W_{\text{pl},y}k_{y,\theta}(f_y/\gamma_{M,\text{fi}})} \leqslant 1 \tag{9}$$

with

$$K_{\text{LT}} = 1 - \frac{\mu_{\text{LT}}N_{\text{fi},\text{Ed}}}{(\chi_{z,\text{fi}}/1.2)Ak_{y,\theta}f_y} \quad \text{but } K_{\text{LT}} \leqslant 1.0 \tag{10}$$

and

$$\mu_{\mathrm{LT}} = 0.15\bar{\lambda}_{z,\theta}\beta_{M,\mathrm{LT}} - 0.15 \quad \text{but } \mu \leqslant 0.9, \tag{11}$$

where $\beta_{M,\mathrm{LT}}$ is the equivalent uniform moment factor corresponding to lateral-torsional buckling, in this case ($\beta_{M,\mathrm{LT}} = \beta_{M,y} = 1.1$).

The reduction factor for lateral-torsional buckling is calculated according to the expressions of Eurocode 3, if the slenderness $\bar{\lambda}_{\mathrm{LT},\theta}$ at the temperature θ exceeds 0.4. The reduction factor in case of fire, $\chi_{\mathrm{LT,fi}}$, is determined like at room temperature using the slenderness $\bar{\lambda}_{\mathrm{LT},\theta}$ given by

$$\bar{\lambda}_{\mathrm{LT},\theta} = \bar{\lambda}_{\mathrm{LT}}\sqrt{\frac{k_{y,\theta}}{k_{E,\theta}}}. \tag{12}$$

Again, in order to compare the results, the maximum value of the design moment is divided by the plastic moment resistance at temperature θ. Solving for $M_{y,\mathrm{fi,Ed}}$ from Eq. (9) and dividing by $M_{y,\mathrm{fi},\theta,\mathrm{Rd}}$ from Eq. (7), gives

$$\frac{M_{y,\mathrm{fi,Ed}}}{M_{y,\mathrm{fi},\theta,\mathrm{Rd}}} \leqslant \frac{\chi_{\mathrm{LT}}}{1.2\left(1 - \dfrac{\mu_{\mathrm{LT}}N_{\mathrm{fi,Ed}}}{(\chi_{z,\mathrm{fi}}/1.2)N_{\mathrm{fi},\theta,\mathrm{Rd}}\gamma_{M,\mathrm{fi}}}\right)}$$
$$\times \left(1 - \frac{N_{\mathrm{fi,Ed}}}{(\chi_{z,\mathrm{fi}}/1.2)N_{\mathrm{fi},\theta,\mathrm{Rd}}}\right). \tag{13}$$

3.3. Simple model according to the new version of Eurocode 3 (2002)

According to the new version of Eurocode 3 [4] the elements with cross-sectional classes Sections 1 and 2 subjected to bending and axial compression, in case of fire, must satisfy the condition:

$$\frac{N_{\mathrm{fi,Ed}}}{\chi_{\mathrm{min,fi}}Ak_{y,\theta}(f_y/\gamma_{M,\mathrm{fi}})} + \frac{K_y M_{y,\mathrm{fi,Ed}}}{W_{\mathrm{pl},y}k_{y,\theta}(f_y/\gamma_{M,\mathrm{fi}})} \leqslant 1, \tag{14}$$

where

$$K_y = 1 - \frac{\mu_y N_{\mathrm{fi,Ed}}}{\chi_{y,\mathrm{fi}}Ak_{y,\theta}(f_y/\gamma_{M,\mathrm{fi}})} \quad \text{but } K_y \leqslant 3 \tag{15}$$

and

$$\mu_y = (1.2\beta_{M,y} - 3)\bar{\lambda}_{y,\theta} + 0.44\beta_{M,y} - 0.29$$
$$\text{but } \mu \leqslant 0.8 \tag{16}$$

with

$$\chi_{\mathrm{fi}} = \frac{1}{\phi_\theta + \sqrt{[\phi_\theta]^2 - [\bar{\lambda}_\theta]^2}}, \tag{17}$$

where

$$\phi_\theta = \frac{1}{2}[1 + \alpha\bar{\lambda}_\theta + (\bar{\lambda}_\theta)^2] \tag{18}$$

and

$$\alpha = 0.65\sqrt{235/f_y} \tag{19}$$

χ_{fi} is the reduction factor to the axis yy and zz in case of fire;

$$\bar{\lambda}_{y,\theta} = \bar{\lambda}_y\sqrt{\frac{k_{y,\theta}}{k_{E,\theta}}}, \quad \bar{\lambda}_{z,\theta} = \bar{\lambda}_z\sqrt{\frac{k_{y,\theta}}{k_{E,\theta}}} \tag{20}$$

with $\bar{\lambda}_y$ e $\bar{\lambda}_z$ are the slenderness of the axis yy and zz at room temperature; $k_{E,\theta}$ the reduction factor of the elastic modulus at temperature θ.

Following the same strategy as before, solving for $M_{y,fi,Ed}$ from Eq. (14) and dividing by $M_{y,fi,\theta,Rd}$ from Eq. (7), yields the ratio of applied moment versus resisting moment for a given level of axial force:

$$\frac{M_{y,fi,Ed}}{M_{y,fi,\theta,Rd}} \leqslant \frac{1}{(1 - (\mu_y N_{fi,Ed}/\chi_{y,fi} N_{fi,\theta,Rd}))}$$
$$\times \left(1 - \frac{N_{fi,Ed}}{\chi_{min,fi} N_{fi,\theta,Rd}}\right) \tag{21}$$

Again, the lateral-torsional buckling check is given by

$$\frac{N_{fi,Ed}}{\chi_{z,fi} A k_{y,\theta}(f_y/\gamma_{M,fi})}$$
$$+ \frac{K_{LT} M_{y,fi,Ed}}{\chi_{LT,fi} W_{pl,y} k_{y,\theta}(f_y/\gamma_{M,fi})} \leqslant 1, \tag{22}$$

where

$$K_{LT} = 1 - \frac{\mu_{LT} N_{fi,Ed}}{\chi_{z,fi} A k_{y,\theta}(f_y/\gamma_{M,fi})} \quad \text{but } K_{LT} \leqslant 1.0 \tag{23}$$

and

$$\mu_{LT} = 0.15\bar{\lambda}_{z,\theta}\beta_{M,LT} - 0.15 \quad \text{but } \mu \leqslant 0.9, \tag{24}$$

where $\beta_{M,LT}$ is the equivalent uniform moment factor corresponding to lateral-torsional buckling, in this case ($\beta_{M,LT} = \beta_{M,y} = 1.1$); where

$$\chi_{LT,fi} = \frac{1}{\phi_{LT,\theta} + \sqrt{[\phi_{LT,\theta}]^2 - [\bar{\lambda}_{LT,\theta}]^2}} \tag{25}$$

with

$$\phi_{LT,\theta} = \frac{1}{2}[1 + \alpha\bar{\lambda}_{LT,\theta} + (\bar{\lambda}_{LT,\theta})^2], \tag{26}$$

$$\alpha = 0.65\sqrt{235/f_y} \tag{27}$$

and

$$\bar{\lambda}_{\text{LT},\theta} = \bar{\lambda}_{\text{LT}}\sqrt{k_{\text{y},\theta}/k_{\text{E},\theta}}. \tag{28}$$

Similarly, for comparison, the maximum value of the design moment (taken from Eq. (22)) is divided by the plastic moment resistance at temperature (Eq. (7)), to give

$$\frac{M_{y,\text{fi,Ed}}}{M_{\text{fi},\theta,\text{Rd}}} \leqslant \frac{\chi_{\text{LT}}}{(1 - (\mu_{\text{LT}}N_{\text{fi,Ed}}/\chi_{z,\text{fi}}N_{\text{fi},\theta,\text{Rd}}))}$$
$$\times \left(1 - \frac{N_{\text{fi,Ed}}}{\chi_{z,\text{fi}}N_{\text{fi},\theta,\text{Rd}}}\right). \tag{29}$$

4. Comparative analysis of the numerical results and the two versions of Eurocode 3

4.1. Basic results: steel members loaded in compression or in bending

To establish the grounds for the subsequent analysis of the behaviour of beam-columns, it is worth recalling the results of axially compressed columns and simply supported beams loaded in pure bending under fire conditions.

For both versions of part 1.2 of Eurocode 3, Fig. 3 compares the axial resistance of an axially compressed pin-ended column, non-dimensionalised with respect to its plastic resistance, for a range of non-dimensional slenderness, $\bar{\lambda}_{\text{LT},\theta}$, with the corresponding numerical results for various constant temperature simulations (400–700°C). It is noted that, although the numerical results apparently highlight a slight unconservative nature of the Eurocode design expressions, experimental results indicate otherwise, an issue briefly discussed in the Section 5.

Analogously, Fig. 4 compares the non-dimensional bending resistance of a simply supported beam under equal end moments from the two Eurocodes proposals, against the numerical results obtained using the program SAFIR for a range of uniform temperatures from 400°C to 700°C, for various levels of non-dimensional slenderness, $\bar{\lambda}_{\text{LT},\theta}$. In this case, the more recent Eurocode design proposal provides perfect fit to the numerical results.

4.2. Beam-column results: combined major-axis bending and axial force

In order to assess the Eurocode design rules for bending and axial force, a parametric study was carried out where the following parameters were considered:

 (i) length of beam-column, L;
 (ii) level of axial force, $N/N_{\text{fi},\theta,\text{Rd}}$;
(iii) temperature.

For each length L, and for a chosen temperature, the Eurocode design Expressions (13) and (29) were plotted for increasing ratios of $N/N_{\text{fi},\theta,\text{Rd}}$, together with the results
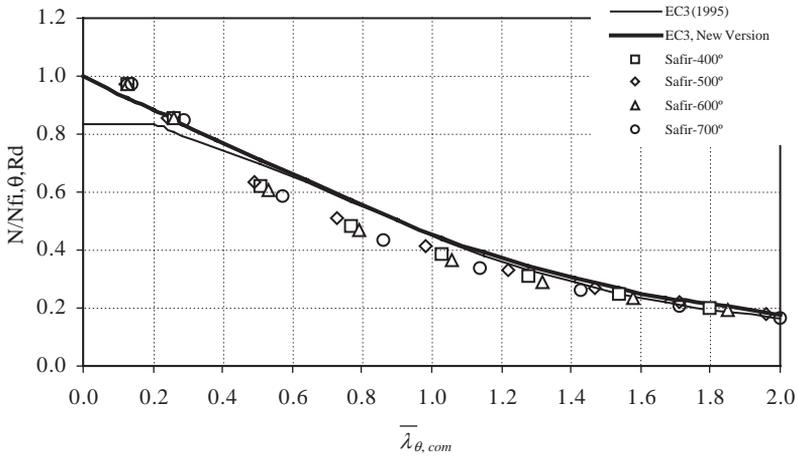
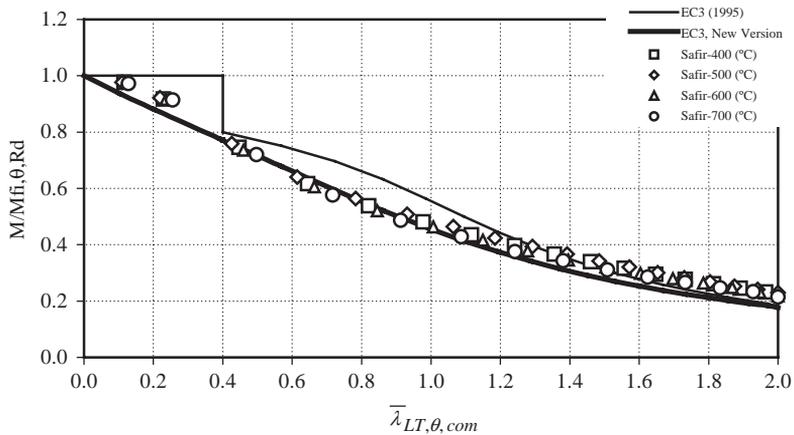Fig. 3. Design curves for buckling of columns.

Fig. 4. Design curves for lateral torsional buckling of beams.

of the numerical simulations for that beam-column length. These results are illustrated in the charts of Figs. 5 and 6, for uniform temperatures of 400°C and 600°C.

Overall, it can be seen that the Eurocode results are mostly on the safe side, as can be summarized in the 3D interaction surfaces of Figs. 7–10. In each figure, the continuous surface corresponds to the simple model of Eurocode whereas the cross points result from the numerical simulations, only visible over the surface, i.e. when the simple model is on the safe side. These figures clearly show that there are more points in the safe side for the newer version.
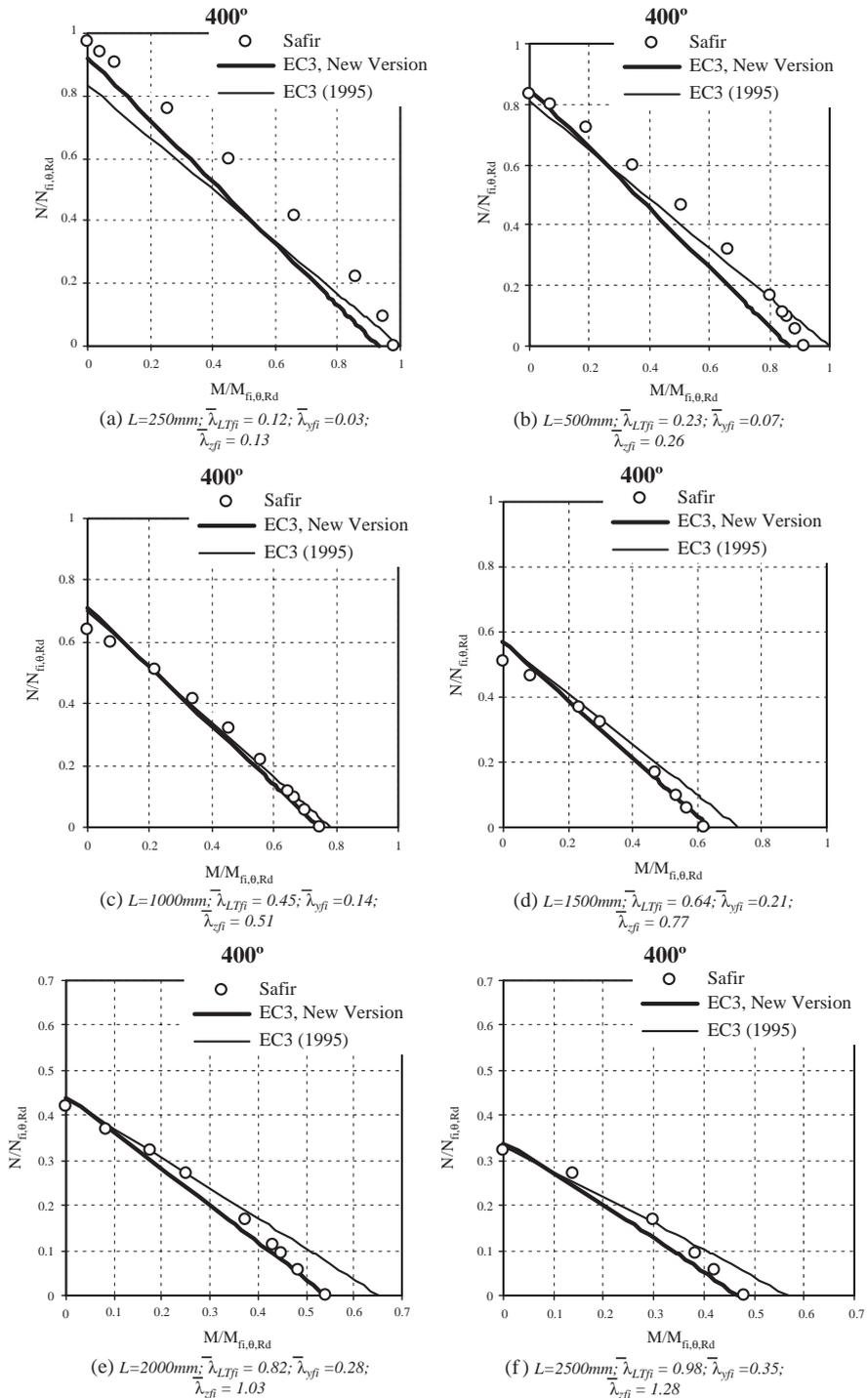
(a) *L=250mm;* $\overline{\lambda}_{LTfi} = 0.12$; $\overline{\lambda}_{yfi} = 0.03$; $\overline{\lambda}_{zfi} = 0.13$

(b) *L=500mm;* $\overline{\lambda}_{LTfi} = 0.23$; $\overline{\lambda}_{yfi} = 0.07$; $\overline{\lambda}_{zfi} = 0.26$

(c) *L=1000mm;* $\overline{\lambda}_{LTfi} = 0.45$; $\overline{\lambda}_{yfi} = 0.14$; $\overline{\lambda}_{zfi} = 0.51$

(d) *L=1500mm;* $\overline{\lambda}_{LTfi} = 0.64$; $\overline{\lambda}_{yfi} = 0.21$; $\overline{\lambda}_{zfi} = 0.77$

(e) *L=2000mm;* $\overline{\lambda}_{LTfi} = 0.82$; $\overline{\lambda}_{yfi} = 0.28$; $\overline{\lambda}_{zfi} = 1.03$

(f) *L=2500mm;* $\overline{\lambda}_{LTfi} = 0.98$; $\overline{\lambda}_{yfi} = 0.35$; $\overline{\lambda}_{zfi} = 1.28$

Fig. 5. Interaction diagrams for combined moment and axial load at 400°C.

(g) $L=3000mm; \overline{\lambda}_{LTfi} = 1.12; \overline{\lambda}_{yfi} =0.42;$
$\overline{\lambda}_{zfi} = 1.54$

(h) $L=3500mm; \overline{\lambda}_{LTfi} = 1.24; \overline{\lambda}_{yfi} =0.49;$
$\overline{\lambda}_{zfi} = 1.80$

(i) $L=4000mm; \overline{\lambda}_{LTfi} = 1.35; \overline{\lambda}_{yfi} =0.56;$
$\overline{\lambda}_{zfi} = 2.05$

(j) $L=4500mm; \overline{\lambda}_{LTfi} = 1.46; \overline{\lambda}_{yfi} =0.63;$
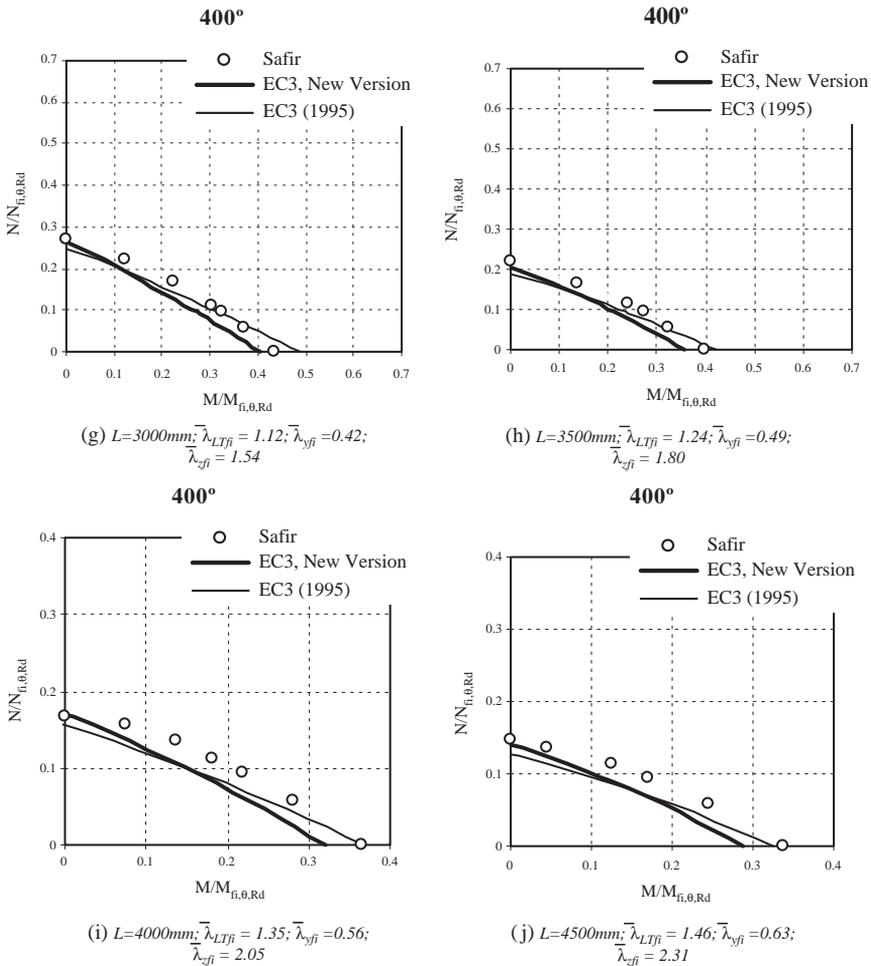$\overline{\lambda}_{zfi} = 2.31$

Fig. 5 (*continued*).

5. Conclusions

The comparative analysis performed in this paper has shown that for the beam-column IPE 220 studied with length varying between 0.5 and 4.5 m, the new version for the fire part of Eurocode is safer than the ENV version from 1995. Although the numerical study presented here was limited to a single section size (IPE 220) and steel class (S235), a previous parametric study for different steel sections and steel grades performed for lateral-torsional buckling of steel beams subjected to fire loading [5,6,15] highlighted no qualitative changes, thus justifying the extrapolation of these results. Analogously, the influence of temperature gradients across the web and flanges, also studied in the context of the lateral-torsional buckling behaviour of steel
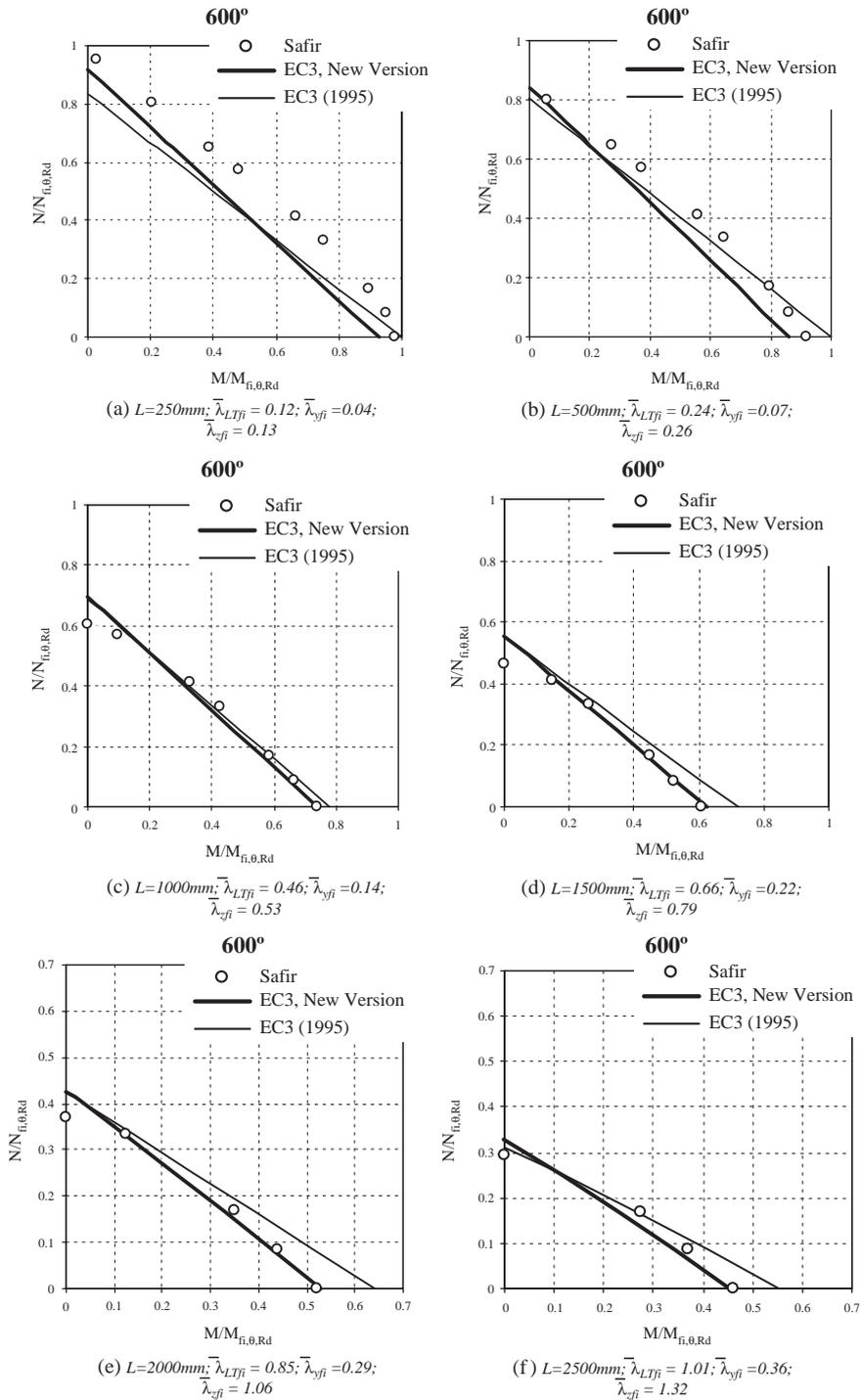
(a) $L=250mm; \overline{\lambda}_{LTfi} = 0.12; \overline{\lambda}_{yfi} = 0.04;$
$\overline{\lambda}_{zfi} = 0.13$

(b) $L=500mm; \overline{\lambda}_{LTfi} = 0.24; \overline{\lambda}_{yfi} = 0.07;$
$\overline{\lambda}_{zfi} = 0.26$

(c) $L=1000mm; \overline{\lambda}_{LTfi} = 0.46; \overline{\lambda}_{yfi} = 0.14;$
$\overline{\lambda}_{zfi} = 0.53$

(d) $L=1500mm; \overline{\lambda}_{LTfi} = 0.66; \overline{\lambda}_{yfi} = 0.22;$
$\overline{\lambda}_{zfi} = 0.79$

(e) $L=2000mm; \overline{\lambda}_{LTfi} = 0.85; \overline{\lambda}_{yfi} = 0.29;$
$\overline{\lambda}_{zfi} = 1.06$

(f) $L=2500mm; \overline{\lambda}_{LTfi} = 1.01; \overline{\lambda}_{yfi} = 0.36;$
$\overline{\lambda}_{zfi} = 1.32$

Fig. 6. Interaction diagrams for combined moment and axial load at 600°C.

600°

(g) $L=3000mm; \overline{\lambda}_{LTfi} = 1.15; \overline{\lambda}_{yfi} = 0.43;$
$\overline{\lambda}_{zfi} = 1.59$

600°

(h) $L=3500mm; \overline{\lambda}_{LTfi} = 1.28; \overline{\lambda}_{yfi} = 0.50;$
$\overline{\lambda}_{zfi} = 1.85$

600°

(i) $L=4000mm; \overline{\lambda}_{LTfi} = 1.40; \overline{\lambda}_{yfi} = 0.58;$
$\overline{\lambda}_{zfi} = 2.12$

600°

(j) $L=4500mm; \overline{\lambda}_{LTfi} = 1.50; \overline{\lambda}_{yfi} = 0.65;$
$\overline{\lambda}_{zfi} = 2.38$
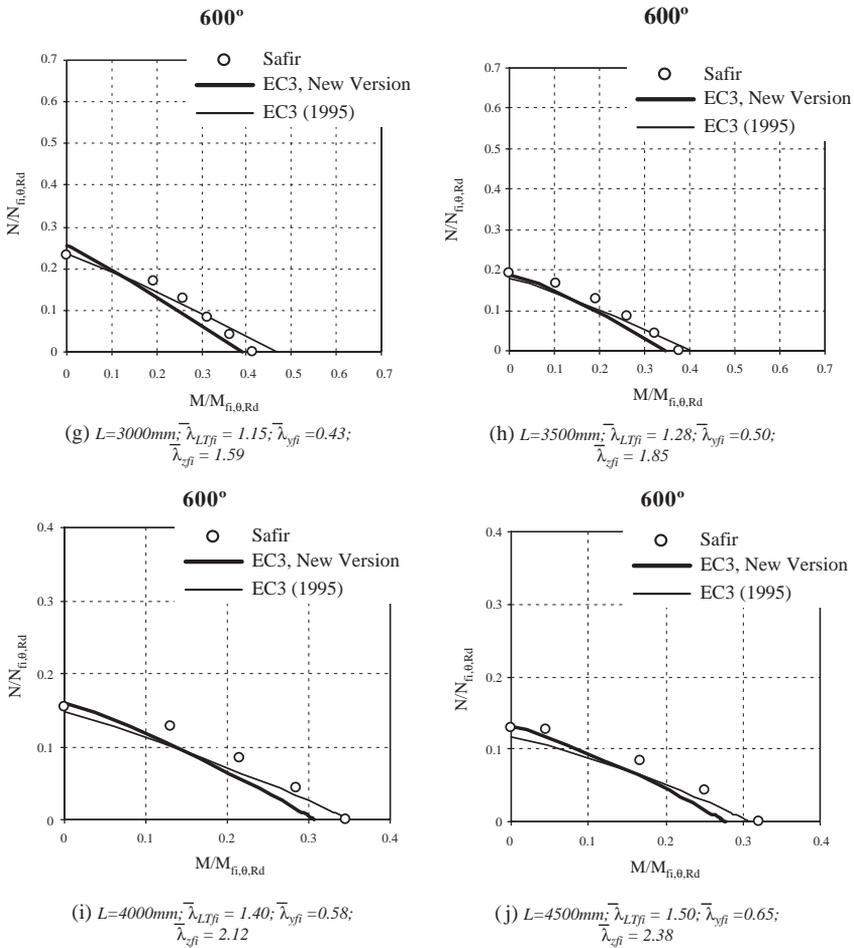
Fig. 6 (*continued*).

beams [5,6] was chosen to have a negligible effect on the resistance of beams and was disregarded in the present study.

　　This new proposal is general on the safe side when compared to numerical results, as would be expected from a simple calculation model. This is not systematically the case, especially for short members submitted mainly to axial forces. It has yet to be mentioned that Franssen et al. [2] have calibrated the simple model against experimental tests results in case of a 2D behaviour (no lateral torsional buckling) and have shown that it is very much on the safe side to perform numerical analyses that consider simultaneously a characteristic value for both imperfections, namely the geometrical out of straightness and the residual strength. It can thus reasonably be expected that the simple model would prove to be on the safe side for the whole
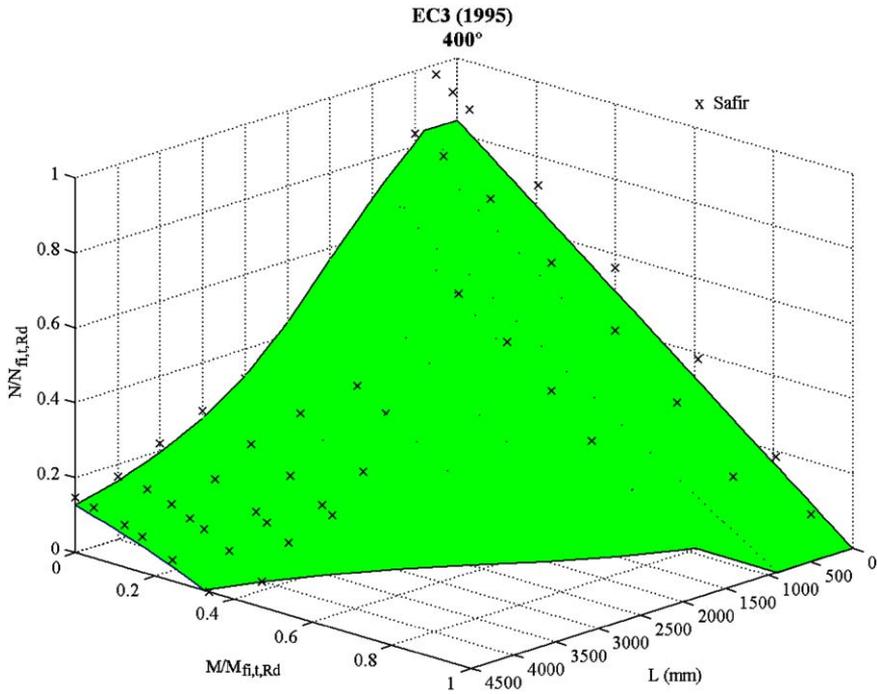
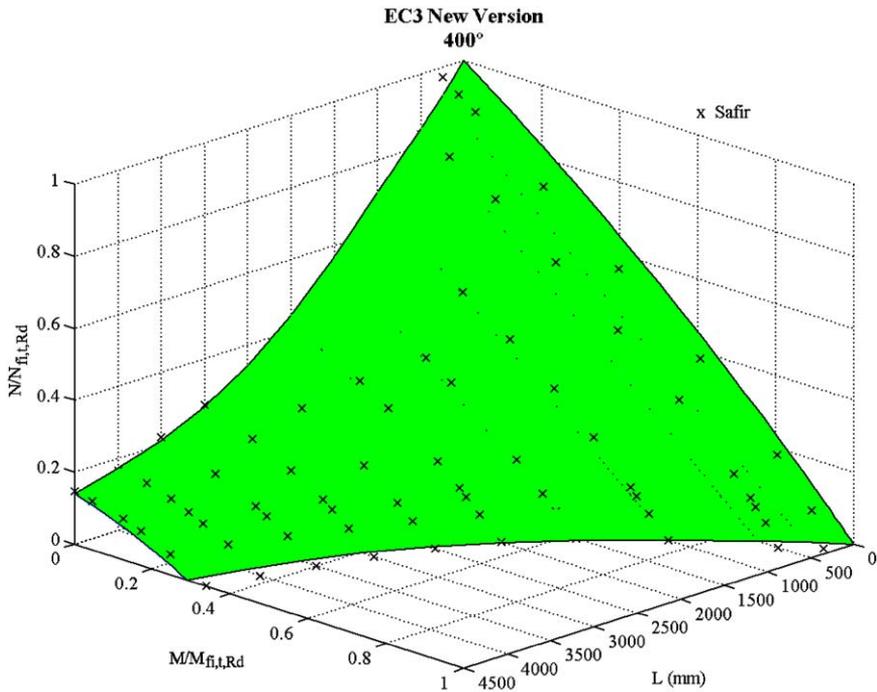Fig. 7. Interaction surfaces for combined moment and axial load at 400°C—version from 1995.

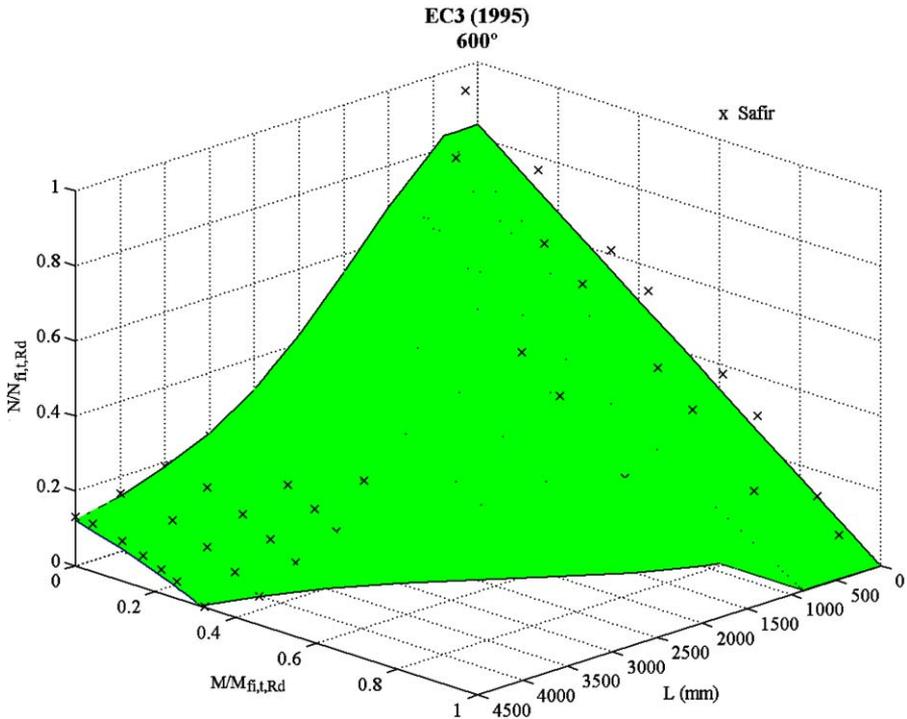Fig. 8. Interaction surfaces for combined moment and axial load at 400°C—new version.

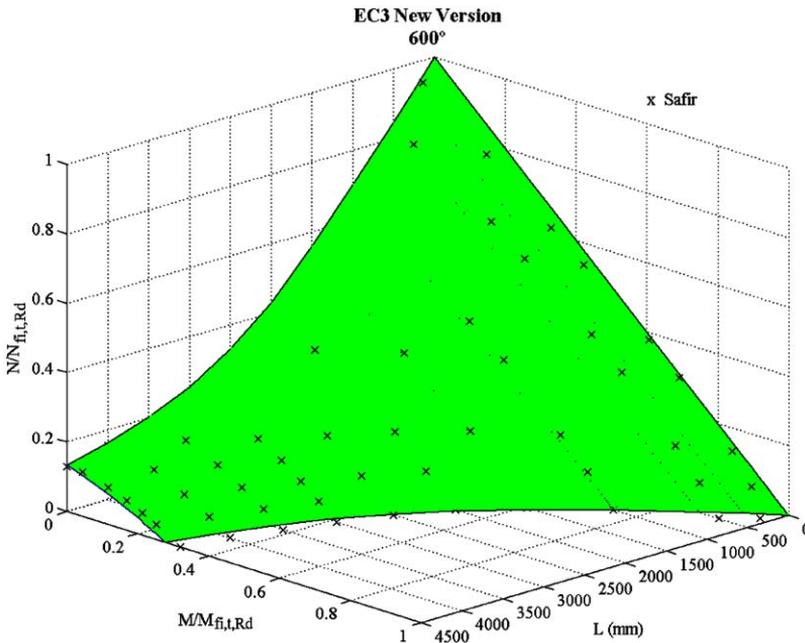Fig. 9. Interaction surfaces for combined moment and axial load at 600°C—version from 1995.

Fig. 10. Interaction surfaces for combined moment and axial load at 600°C—new version.

(M,N,L) range if compared to experimental tests. Such tests involving 3D behaviour in elements submitted to axial force and bending moment at elevated temperature have yet to be performed.

References

[1] Franssen J-M, Schleich J-B, Cajot L-G. A simple model for fire resistance of axially loaded members according to Eurocode 3. J Constr Steel Res 1995;35:49–69.

[2] Franssen J-M, Schleich J-B, Cajot L-G, Azpiazu WA. Simple model for the fire resistance of axially loaded members—comparison with experimental results. J Constr Steel Res 1996;37:175–204.

[3] Franssen JM, Taladona D, Kruppa J, Cajot LG. Stability of steel columns in case of fire: experimental evaluation. J Struct Eng 1998;124(2):158–63.

[4] Eurocode 3, Design of steel structures—part 1–2. General rules—structural fire design. Draft prEN 1993-1-2:20xx, Stage 34, European Committee for Standardisation, Brussels, Belgium, February 2002.

[5] Vila Real PMM, Franssen J-M. Lateral buckling of steel I beams under fire conditions—Comparison between the EUROCODE 3 and the SAFIR code, Internal Report No. 99/02, Institute of Civil Engineering—Service Ponts et Charpents—of the University of Liege, 1999.

[6] Vila Real PMM, Franssen J-M. Numerical modelling of lateral buckling of steel I beams under fire conditions—Comparison with Eurocode 3. J Fire Prot Eng, USA 2001;11(2):112–28.

[7] Vila Real PMM, Piloto PAG, Franssen J-M. A new proposal of a simple model for the lateral-torsional buckling of unrestrained steel I-beams in case of fire: experimental and numerical validation. J Constr Steel Res 2003;59/2:179–99.

[8] Franssen J-M, Kodur VKR, Mason J. User's manual for SAFIR (Version NZ). A Computer program for analysis of structures submitted to the fire. University of Liege, Ponts et Charpentes, Rapport interne SPEC/2000_03, 2000.

[9] Eurocode 3, Design of steel structures—part 1–1. General rules and rules for buildings. ENV 1993-1-1. Brussels, Belgium: Commission of the European Communities; 1992.

[10] Franssen J-M. Modelling of the residual stresses influence in the behaviour of hot-rolled profiles under fire conditions. Constr Mét 1989;3:35–42 (in French).

[11] Franssen JM. The unloading of building materials submitted to fire. Fire Safety J 1990;16:213–27.

[12] Souza V, Franssen J-M. Lateral buckling of steel I beams at elevated temperature—comparison between the modelling with beam and shell elements. In: Lamas A, Simões da Silva L, editors. Proceeding of the Third European Conference on Steel Structures. Coimbra: Univ. de Coimbra; 2002, p. 1479–88, ISBN 972-98376-3-5.

[13] ECCS—European Convention for Constructional Steelwork, Technical committee 8—structural stability, technical working group 8.2—system, ultimate limit state calculation of sway frames with rigid joints, 1st ed. 1984.

[14] Eurocode 3, Design of steel structures—part 1–2. General rules—structural fire design. ENV 1993-1-2. Brussels, Belgium: European Committee for Standardisation; 1995.

[15] Cazeli R, Vila Real PMM, Silva VP, Piloto PAG. Numerical modelling of the lateral-torsional buckling of steel I-beam under fire conditions. A contribution to validate a new proposal for Part 1.2 of the Eurocode 3. São Paulo, Brasil: I Congresso Internacional da Construção Metálica—I CICOM; 2001 (in Portuguese).

[16] Chen WF, Lui EM. Structural stability—theory and implementation. New York: Elsevier; 1987.